Published in
Review of Scientific Instruments 82, issue 123116, 1-11, 2011
which should be used for any reference to this work

Frequency discriminators for the characterization of narrow-spectrum heterodyne beat signals: Application to the measurement of a sub-hertz carrier-envelope-offset beat in an optical frequency comb

Stéphane Schilt,[1,a)] Nikola Bucalovic,[1] Lionel Tombez,[1] Vladimir Dolgovskiy,[1] Christian Schori,[1] Gianni Di Domenico,[1] Michele Zaffalon,[2] and Pierre Thomann[1]

[1]*Laboratoire Temps-Fréquence, Université de Neuchâtel, Avenue de Bellevaux 51, CH-2000 Neuchâtel, Switzerland*
[2]*Zurich Instruments Ltd, Technoparkstrasse 1, CH-8005 Zürich, Switzerland*

We describe a radio-frequency (RF) discriminator, or frequency-to-voltage converter, based on a voltage-controlled oscillator phase-locked to the signal under test, which has been developed to analyze the frequency noise properties of an RF signal, e.g., a heterodyne optical beat signal between two lasers or between a laser and an optical frequency comb. We present a detailed characterization of the properties of this discriminator and we compare it to three other commercially available discriminators. Owing to its large linear frequency range of 7 MHz, its bandwidth of 200 kHz and its noise floor below 0.01 Hz^2/Hz in a significant part of the spectrum, our frequency discriminator is able to fully characterize the frequency noise of a beat signal with a linewidth ranging from a couple of megahertz down to a few hertz. As an example of application, we present measurements of the frequency noise of the carrier envelope offset beat in a low-noise optical frequency comb.

I. INTRODUCTION

Narrow-linewidth and highly stable lasers, such as extended cavity diode lasers (ECDL) (Ref. 1) stabilized to an external frequency reference (usually a Fabry–Perot cavity or a molecular/atomic transition) are routinely used nowadays in various applications, such as high-resolution spectroscopy, coherent optical communications, or atomic physics to name a few. In frequency metrology, the advent of optical atomic clocks that have surpassed the best microwave primary frequency standards in terms of stability,[2] has led to the development of a new class of ultra-stable lasers with a linewidth at the hertz level[3] or even better.[4,5] Such performances are obtained by tightly locking a laser with good free-running frequency noise properties (usually an ECDL) to an ultra-high finesse Fabry–Perot resonator using the Pound–Drever–Hall stabilization method.[6] To achieve such a narrow linewidth, the initial frequency noise characteristics of the free-running laser have to be known in order to properly design the servo-loop filter that is needed, in conjunction with the cavity resonance error signal, to generate the laser feedback signal. Additionally, it is necessary to characterize the residual frequency noise properties of the locked laser.

The spectral properties of a laser can be conveniently described either in terms of its optical line shape and associated linewidth or in terms of its frequency noise power spectral density (PSD). The optical linewidth (usually described as the full width at half maximum—FWHM—of the line-shape function) is a single parameter that is often used to characterize the spectral properties of a laser. The linewidth can be determined, e.g., by self-homodyne/heterodyne interferometry using a long fiber delay line.[7] However, heterodyning with another laser of similar spectral properties, or even with a reference source of narrower linewidth, is the traditional approach for ultra-narrow linewidth lasers, as self-homodyne/heterodyne methods are inapplicable due to the extremely long delay line that would be required. Describing the spectral properties of a laser by its linewidth is convenient, as it allows an easy and straightforward comparison between different laser sources. But this single number gives an incomplete picture of the actual laser frequency noise as, e.g., it does not give any information about the spectral distribution of the noise, which is of prime importance when one aims at identifying possible sources of external perturbations (e.g., acoustic noise, power-line-induced noise, etc.) affecting a laser.[8] Furthermore, the common frequency noise characteristics of a free-running laser with flicker noise diverging at low frequency leads to a linewidth that depends on the observation time, making it improper as a figure of merit of the laser spectral properties. On the other hand, the knowledge of the frequency noise PSD provides a complete picture of the laser frequency noise, showing, e.g., at which frequency the dominant noise that contributes to the laser linewidth occurs. Such knowledge is in particular important to determine the feedback bandwidth that is needed to narrow the laser linewidth down to the required level.[9]

In this paper, we present a frequency discriminator that we have developed to measure the frequency noise of a radio-frequency (RF) beat signal, as well as different commercially available discriminators, that we have also characterized for comparison. A detailed characterization of these discriminators is presented in Sec. II, in terms of various relevant parameters, such as their sensitivity, bandwidth, and noise floor. Based on these results, the range of operation of the

a)Electronic mail: stephane.schilt@unine.ch.

discriminators are determined and compared. Then, an example of application is shown in Sec. III, where the different discriminators are compared to analyze the frequency noise of a real heterodyne beat signal, which is the carrier envelope offset (CEO) beat signal in an optical frequency comb.[11]

II. FREQUENCY DISCRIMINATORS

In order to measure the frequency noise spectrum of a laser, a suitable frequency-to-voltage converter (also referred to as a frequency discriminator) must be available, which converts frequency fluctuations of the laser into fluctuations of an electrical signal (voltage) that can be spectrally analyzed, e.g., using a fast Fourier transform (FFT) analyzer. Basically, frequency discriminators can be split into two categories: optical discriminators and RF discriminators. *Optical frequency discriminators* directly convert optical frequency fluctuations of the laser into intensity fluctuations that are detected by a photodetector. Optical discriminators are typically devices displaying a frequency-dependent transmission in a restricted frequency range, such as gas-filled cells near an atomic/molecular resonance (Doppler-broadened[10–12] or sub-Doppler[13]), Fabry–Perot resonators[14] or unbalanced two-beam interferometers.[15]

As it is not always possible to have a proper optical discriminator at the considered laser wavelength, another approach consists in heterodyning the laser under test with a second laser, either similar to the first one or with a negligible frequency noise, and subsequently analyzing the generated RF beat signal. In the first case, the two lasers are considered to contribute equally to the noise of the RF beat and the frequency noise PSD of the beat signal is (at most) twice that of a single laser. In the second case, the frequency noise PSD of the laser under test is directly obtained since the noise of the reference laser is much smaller. The frequency noise of the heterodyne beat can be analyzed in the frequency domain using a suitable *RF frequency discriminator*. In this work, we will discuss the use of different types of RF frequency discriminators that we have evaluated.

A frequency discriminator is characterized by its sensitivity (or discrimination slope D_ν in [V/Hz]), i.e., its ability to convert frequency fluctuations $\delta\nu(t)$ of the input signal into variations of an output voltage $V(t)$. The discriminator slope is an important parameter: the higher D_ν, the better the frequency noise conversion. The frequency noise PSD of the input signal ($S_{\delta\nu}(f)$ in [Hz^2/Hz], where f is the Fourier frequency) is retrieved from the PSD of the output voltage ($S_V(f)$ in [V^2/Hz]) taking into account the discriminator slope

$$S_{\delta\nu}(f) = \frac{S_V(f)}{D_\nu^2}. \tag{1}$$

A. Description of the RF frequency discriminators

In this work, we present a frequency discriminator based on an analog phase-locked loop (PLL) that we have developed and compare it with three commercially available frequency discriminators. We first describe here the principle of operation of each discriminator. Then a characterization of several relevant properties of these discriminators will follow in Sec. II B.

1. Analog phase-locked loop discriminator

Following the work of Turner *et al.*,[8] we built an analog PLL frequency discriminator and characterized it in detail. The basic principle of this discriminator is to phase-lock a voltage-controlled oscillator (VCO) to the RF beat signal to be analyzed, using a high-bandwidth PLL. If the loop bandwidth is sufficient, the VCO follows any frequency fluctuations $\delta\nu(t)$ of the input RF beat and the control voltage of the VCO $V(t)$ reflects the frequency fluctuations of the input signal. Once the response of the VCO is known (in [Hz/V]), the analysis of the fluctuations of the control voltage can be directly converted into frequency fluctuations of the input RF beat (within the loop bandwidth). While Turner *et al.* used a single integrated circuit PLL for their frequency discriminator, we built our PLL discriminator using discrete off-the-shelf analog components (VCO, phase detector and servo controller). This approach offers a larger flexibility in the adjustment of the PLL parameters (gain, bandwidth), which enables us to optimize the PLL characteristics with respect to the properties of the signal under test (e.g., to achieve the largest bandwidth or the lowest noise floor). A scheme of the PLL discriminator is shown in Fig. 1. The VCO (Mini-Circuits ZX95-209-S+) operates in the 199–210 MHz range, with a nominal tuning coefficient of 1.5 MHz/V. A double-balanced mixer (Mini-Circuits ZP-1LH) is used as a phase detector, followed by a 10-MHz low-pass filter to suppress high frequency components. Finally, the loop is closed with a high-speed servo controller (New-Focus LB1005-S) with a proportional-integral (PI) corner frequency adjustable from 10 Hz up to 1 MHz and a proportional gain between -40 dB and $+40$ dB.

2. Miteq RF discriminator

Simple plug-and-play RF discriminators are commercially available in different frequency ranges from various suppliers of radio-frequency components. We tested such a device (Miteq FMDM 21.4/2-4) operating in the range of 18–26 MHz with a typical peak-to-peak bandwidth of 8 MHz and a linear bandwidth of 4 MHz as specified by the manufacturer.[16] The operation of this discriminator is based on the use of an input limiting amplifier to drive two staggered tuned L-C circuits. Opposing rectification of the circuits creates the discriminator 'S' curve and a video amplifier is finally utilized to provide adequate output slope. The ability to precisely align the skirts of the tuned circuits, which represents the discriminator linear bandwidth, is an advantage of this type of design. The nominal response of this discriminator is 1 V/MHz.

3. Numerical phase-locked loop HF2PLL discriminator

The HF2LI from Zurich Instruments, Switzerland, is an all-numerical instrument consisting of a dual input digital lock-in amplifier extended with dual PLL capabilities.[17] The

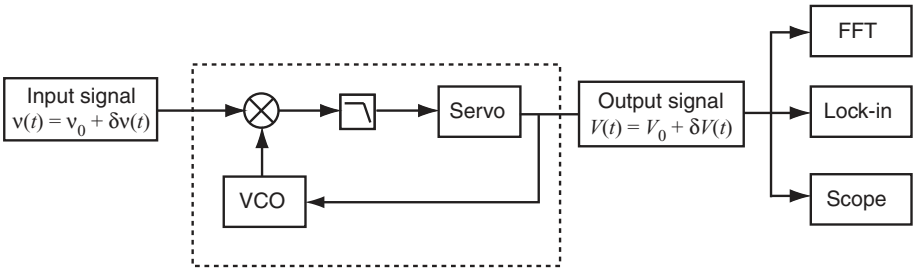

FIG. 1. Schematic representation of our analog PLL discriminator. The control voltage $V(t)$ of the VCO constitutes the output signal that replicates the input frequency variations $\delta\nu(t)$. This signal is analyzed using an oscilloscope, a lock-in amplifier or a FFT analyzer.

lock-in amplifiers have a frequency bandwidth ranging from 1 μHz to 50 MHz (with a sampling rate of 210 Msamples/s), a dynamic reserve of 120 dB and an input voltage noise of $5\text{nV}/\sqrt{\text{Hz}}$. The instrument is based on a field-programmable gate array (FPGA) which permits computations with large numerical precision and short processing time. Moreover, the lock-in shortest integration time constant of 800 ns, lower by one order of magnitude than in other commercially available lock-in amplifiers, makes it suitable for wide bandwidth demodulation and as a phase detector for a PLL (referred to as HF2PLL) that replaces all the analog components in the dotted box in Fig. 1 by their numerical counterparts.

The HF2PLL runs directly on the lock-in FPGA, ensuring a precise control of the PLL dynamics and resulting in a maximum -3 dB bandwidth of 60 kHz. The HF2PLL has similar functional blocks as the analog PLL described in Sec. II A 1, with two notable differences:

(i) The phase detector makes use of the lock-in demodulation chain (including its low pass filters) since its purpose is to determine the phase difference between input and reference signals. This phase difference is the lock-in output channel *Theta*, as calculated directly from the quadrature (Y) and in-phase (X) components of the demodulated signal. The advantage of this approach compared to the analog PLL is its high rejection of amplitude modulations of the input signal, thereby minimizing the amplitude noise sensitivity of the HF2PLL discriminator. *Theta* is the error signal and constitutes the input of the following numerical proportional-integral-derivative (PID) controller, as in the analog case.

(ii) The VCO is replaced by a functionally equivalent numerical controlled oscillator (NCO), whose role is to keep track of the reference signal phase (from which the in-phase and quadrature reference signals are derived). The rate at which the NCO phase changes, which is the reference signal instantaneous frequency, is $f(t) = f_c + dF$, where f_c is a selectable PLL center frequency and the frequency deviation dF (in Hz) is the PID controller output. When the HF2PLL discriminator is used to characterize a heterodyne beat signal, dF is output as an analog signal with a software-selected gain (from 0.75 nV/Hz to 1.6 V/Hz).

In comparison with the analog PLL where all electronic components suffer from $1/f$ and white noise, the noise sources in the digital PLL are confined to the analog-to-digital converter at the lock-in input stage and to the analog dF output, since the numerical noise can be made arbitrarily small by increasing the internal numerical precision. On the other hand, the measurement bandwidth of analog PLLs is usually larger than their digital counterparts.

4. Digital phase detector DXD200

The CEO beat of our optical frequency comb, which will be used to compare the different frequency discriminators, is phase-locked to a 20-MHz frequency reference for self-referencing (see details in Sec. III). For this purpose, a digital phase detector with a wide linear range of operation of $\pm 32 \times 2\pi$ is used to detect the phase fluctuations between the CEO beat and the reference signal, in order to generate the error signal for the stabilization loop. This digital phase detector (DXD200 module from MenloSystems, Germany, which is part of the XPS800 femtosecond phase stabilization unit) has also been used as a diagnostic tool to measure small frequency fluctuations between the signal under test and the reference signal and has been characterized for comparison with the other frequency discriminators.

The basic element of this digital phase detector is a differential period counter, where the reference signal counts up and the RF beat signal counts down.[18] The counter has a range from 0 to 64 and is initialized at 32. The phase error can track a $\pm 32 \times 2\pi$ phase difference between the two signals. The counter signal is then fed into a digital to analog converter to generate a signal proportional to the relative phase, with a nominal phase discrimination factor $D_\varphi = 3.3\text{V}/(32 \times 2\pi) = 0.016$ [V/rad]. While this detector should provide an ideal linear response in a phase range of $\pm 32 \times 2\pi$, this is not the case in reality due to the presence of several nonlinearities in its range of operation. This effect was investigated over the entire range of operation of the phase detector by comparing two signals with a slightly different frequency ($f_1 = f_{\text{ref}} = 20$ MHz, $f_2 = f_1 + \Delta$ with Δ in the range of 10–100 mHz), in order to slowly scan the output voltage (phase difference resulting from the accumulated phase shift between the two signals). Some of the nonlinearities are directly observable in the DC output voltage of the phase detector (see Fig. 2(a)). Next, a small frequency modulation (at a rate $f_{\text{mod}} = 10$ kHz with a span of $\Delta f = 50$ Hz) was applied to one of the 20-MHz carrier in order to measure the frequency response (in amplitude and phase) of the phase

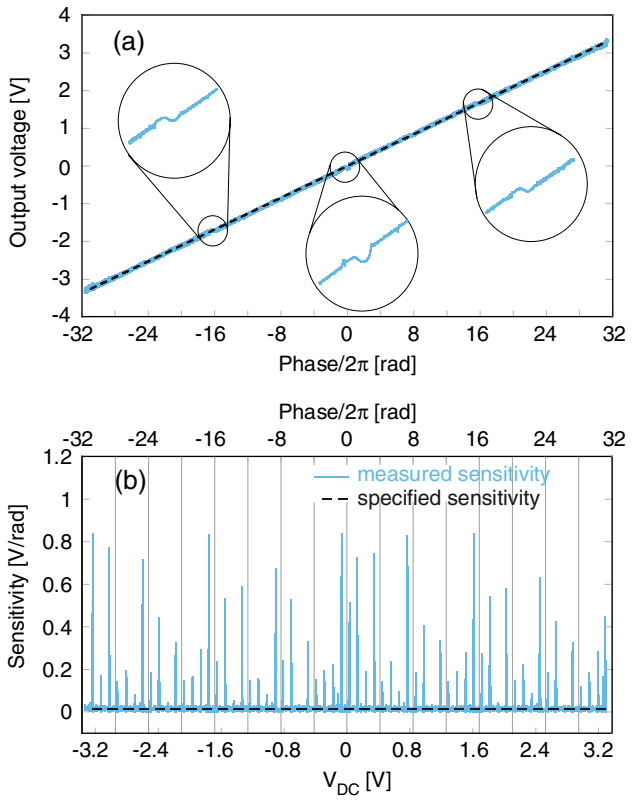

FIG. 2. (Color online) Difference between the ideal (dashed line) and actual (light thick curve) response of the digital phase detector. (a) DC analog output voltage as a function of the phase difference between the two inputs; some nonlinearities are visible at the encircled points. (b) Highlight of the nonlinearities of the detector occurring roughly every 2π phase difference. This curve has been obtained by applying a frequency-modulated carrier at one input of the device and performing lock-in detection at the output to determine the discriminator sensitivity. The dashed line corresponds to the average slope of the DC curve (a).

detector using a lock-in amplifier and to subsequently determine the detector sensitivity (in V/rad), as also described in Sec. II B. In order to be able to resolve the narrow peaks that occur at some specific points in the detector response as a result of the nonlinearities, a small modulation index $\beta = (\Delta f/2)/f_{\rm mod}$ was used. In that case, the measured lock-in signal corresponds to the derivative of the phase detector response and the sensitivity was obtained by normalizing this signal by the modulation depth β. The outputs of the lock-in amplifier (X and Y components) were recorded with an acquisition card (National Instruments NI USB-6008), together with the phase detector operating DC voltage, during a phase sweep. The actual response displayed in Fig. 2(b) is not as smooth as expected and shows the presence of many nonlinearities, regularly separated by a 2π phase difference. At these points, the sensitivity of the detector for small signals can be locally enhanced by a factor up to 50 (0.8 V/rad). In order to have a proper discriminator of known sensitivity, the digital phase detector should be operated at a point where its response is constant, i.e., away from the nonlinear points. All the results shown in the following sections are obtained in such conditions. Finally, we should notice that the DXD200 acts as a phase discriminator, so that the corresponding frequency sensitivity is given by $D_\nu(f) = D_\varphi/f$.

B. Characterization of the frequency discriminators

1. Sensitivity and bandwidth

The sensitivity of each discriminator has been determined by applying a frequency-modulated input signal with a modulation depth $\Delta f = 1$ kHz ($\Delta f = 100$ Hz in the case of the digital phase detector DXD200) at a varying modulation frequency $f_{\rm mod}$ using a calibrated, high-bandwidth reference VCO. A 207-MHz carrier frequency was used with the analog PLL discriminator and a 20-MHz carrier frequency with the other discriminators, obtained by mixing the 207-MHz VCO signal with a 227-MHz reference signal and subsequent low-pass filtering. The modulation frequency $f_{\rm mod}$ was scanned in the range from 0.1 Hz to 10 MHz and the demodulated output signal of the discriminators was measured in amplitude and phase using a lock-in amplifier referenced to $f_{\rm mod}$ (standard lock-in, model Stanford Research Systems SR830, up to 100 kHz and RF lock-in, model SR844, at higher frequency). Finally, the transfer function of each device was obtained by normalizing the lock-in output signal to the input frequency modulation depth Δf. We define here the bandwidth of a discriminator as the frequency range in which the discriminator sensitivity remains within $\pm 10\%$ (± 0.9 dB) of its value at $f_{\rm mod} = 1$ kHz. The sensitivities (or discriminator slopes, in V/Hz) reported throughout this paper are generally given for the discriminator output connected to a high impedance load. The only exception concerns Miteq discriminator, used with a 93-Ω load as specified in the manufacturer's datasheets.

The amplitude and phase of the transfer function of each discriminator are displayed in Fig. 3. The result for the analog PLL is shown for a maximum PI corner frequency of 1 MHz and a PI gain adjusted to optimize the PLL operation. The response of the analog PLL slightly depends on the PLL settings (gain and PI-corner): the low frequency sensitivity is unaffected by the PLL parameters, but at high frequency, the position and amplitude of the oscillation (servo bump) varies with these parameters. The analog PLL has a typical bandwidth of 200 kHz (defined at ± 0.9 dB as mentioned before) with a discriminator slope of 0.7 V/MHz. The Miteq discriminator has the largest bandwidth of 2 MHz with a discriminator slope of 1.25 V/MHz, obtained for 0 dBm input signal, but this sensitivity significantly depends on the signal amplitude (e.g., it is reduced to 0.86 V/MHz at -6 dBm input signal). The HF2PLL has a lower bandwidth of 50 kHz, but its sensitivity is much higher and can be adjusted by software in the range from 0.75 nV/Hz to 1.6 V/Hz. For the Miteq and analog PLL discriminators, an instantaneous response to frequency fluctuations is obtained up to $f_{\rm mod} > 100$ kHz, while a significant phase shift is introduced at higher frequencies. In the HF2PLL, the phase shift occurs at much lower frequency, which is compatible with the amplitude attenuation. The sensitivity of the digital phase detector DXD200 decreases as $1/f$ as the module acts as a phase comparator. The measured phase discriminator is around 0.018 V/rad (0.016 V/rad expected from specifications, corresponding to $D_\varphi = 3.3\text{V}/(32 \times 2\pi)$). The phase detector introduces a -90° phase shift at low Fourier frequency as it acts as a phase detector and we are assessing its response in terms of frequency. At Fourier frequencies higher than 100 kHz, a significantly larger

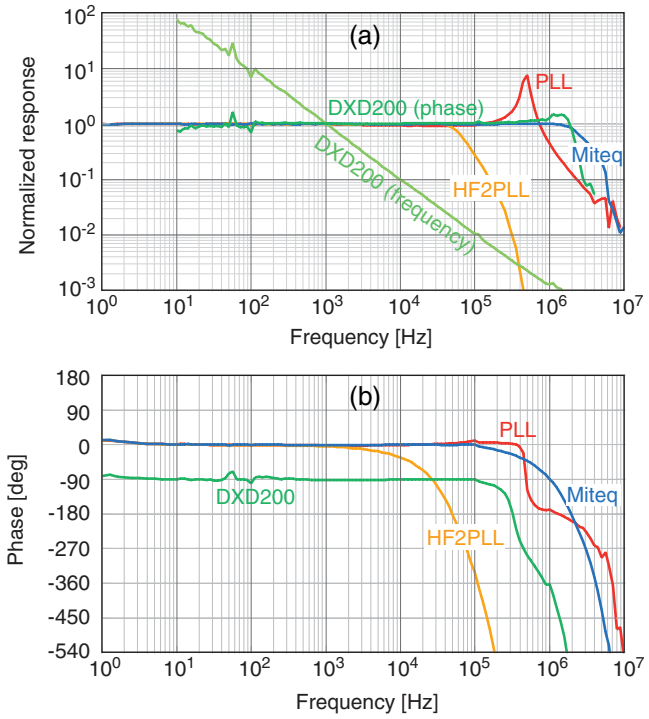

FIG. 3. (Color online) Amplitude (a) and phase (b) of the normalized transfer function of the different discriminators, measured by applying a frequency-modulated input carrier and performing lock-in detection of the discriminator demodulated signal. Each transfer function has been normalized by the discriminator sensitivity measured at 1 kHz modulation frequency ($D_v = 7 \times 10^{-7}$ [V/Hz] for PLL, $D_v = 1.25 \times 10^{-6}$ [V/Hz] for Miteq, $D_v = 10^{-3}$ [V/Hz] for HF2PLL, $D_v = 1.8 \times 10^{-5}$ [V/Hz] or $D_\varphi = 1.8 \times 10^{-2}$ [V/rad] for DXD200). The amplitude response of the digital phase detector DXD200 is represented both in terms of response to frequency and phase modulation.

phase shift appears. The ±0.9 dB bandwidth of DXD200 is ≈1 MHz.

2. Frequency range

We define here the *total frequency range* of each discriminator as the frequency interval in which the discriminator operates, and the *linear frequency range* as the frequency interval in which the response is within ±10% (±0.9 dB) of the discriminator sensitivity determined in Sec. II B 1. The frequency range of each discriminator, measured at 1 kHz modulation frequency, is shown in Fig. 4. Both our analog PLL and the Miteq discriminators have a wide linear frequency range of several megahertz (7 MHz for the analog PLL and 9 MHz for Miteq). For the numerical PLL, the situation is different. The input carrier frequency can be anywhere in the range of ≈1–49 MHz, but the amplitude of the maximum detectable frequency fluctuations around this carrier depends on the selected sensitivity of the demodulator output. As the analog output of the HF2LI instrument is limited to ±10 V, the maximum frequency fluctuation Δf_{max} which can be measured for a sensitivity D_v (in V/Hz) is $\Delta f_{max} = \pm 10\text{V}/D_v$. While a high sensitivity can be selected with the HF2PLL instrument, the drawback is a reduced frequency range.

Finally, the digital phase detector DXD200 can operate at any carrier frequency between 0.5 MHz and more than

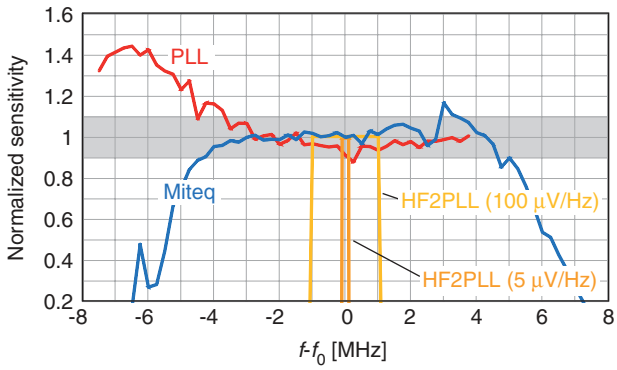

FIG. 4. (Color online) Normalized sensitivity of the frequency discriminators (measured for 1 kHz modulation frequency) as a function of the carrier frequency detuning. The gray area indicates the linear frequency range Δf_{lin} of each discriminator, defined as the frequency interval for which the discriminator response differs by less than ±10% (±0.9 dB) from its nominal sensitivity. The frequency range of the HF2PLL is inversely proportional to the software-selected sensitivity D_v ($\Delta f_{lin} = \pm 10\text{V}/D_v$) and is shown here for two particular cases ($D_v = 100$ μV/Hz and $D_v = 5$ μV/Hz) for illustration.

200 MHz (provided that a reference signal at the same frequency is available), but the range of detectable fluctuations is limited to $\pm 64\pi$ in terms of phase and is thus extremely narrow.

3. Noise floor

A relevant characteristic of a frequency discriminator is its noise floor, which represents the smallest detectable frequency fluctuations with a signal-to-noise ratio of one. The noise floor of the different discriminators was measured with a FFT analyzer for Fourier frequencies up to 100 kHz and with an electrical spectrum analyzer at higher frequencies, when a stable, low-noise carrier was applied to the input. As previously, a 207-MHz carrier was used with the analog PLL discriminator and a 20-MHz carrier frequency with the other discriminators. The PSD of the discriminators output voltage has been converted into frequency noise PSD using the corresponding sensitivities previously determined. Results are shown in Fig. 5.

The noise floor of the analog PLL-discriminator significantly depends on the amplitude of the input signal and on the gain settings of the PI controller. It is presented here for a PI gain adjusted to optimize the noise floor. Operation at too-high gain may increase the noise floor by one or two orders of magnitude at Fourier frequencies above 10 Hz. In the range of 100 Hz–10 kHz, a white frequency noise floor is observed ($\approx 10^{-3}$ Hz^2/Hz). Out of this range, the noise floor scales as f^{-2} at low frequency, resulting from the VCO white frequency noise that is multiplied by f^{-2} due to the Leeson effect[19] and linearly with f at high frequency, resulting from the PLL servo bump.

The noise floor of the Miteq discriminator is white frequency noise (≈0.1 Hz^2/Hz) at frequencies $f >$ 100 Hz and increases as $1/f$ at lower frequency. The digital phase detector DXD200 has a typical $1/f$ phase noise floor, which translates into a small frequency noise floor at low Fourier frequency ($<10^{-5}$ Hz^2/Hz at 10 Hz). The frequency noise floor

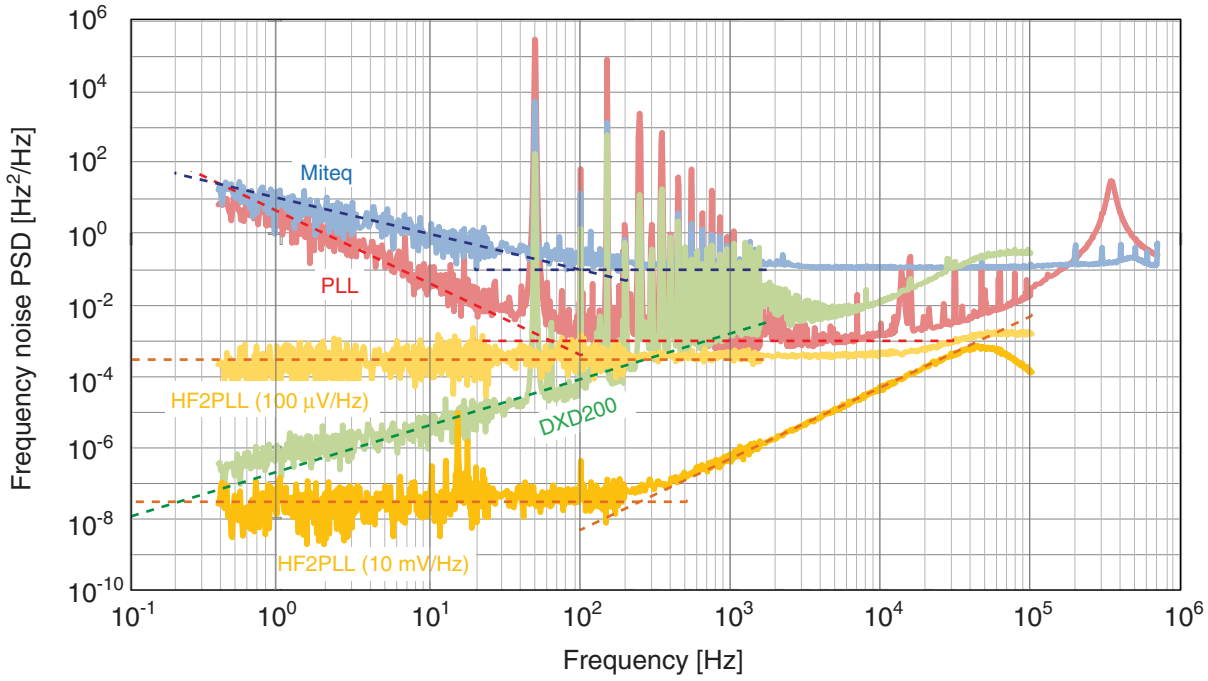

FIG. 5. (Color online) Noise floor of the different discriminators. The noise floor of the analog PLL depends on the PI gain and is presented here in an optimized configuration. The white frequency noise of the HF2PLL (at low frequency) results from white noise at the analog output and thus scales as $1/D_v{}^2$ for sensitivities up to $D_v = 10$ mV/Hz. It is displayed here for two cases, $D_v = 100$ μV/Hz and $D_v = 10$ mV/Hz. The dashed lines represent an approximation of the noise floor of each discriminator in terms of a power series of f (f^{-2}, f^{-1}, f^0, f^1, and f^2).

increases with f with a slope slightly larger than unity in a log-log plot (the experimentally observed dependence is f^α with $\alpha \approx 1.3$), and surpasses the noise floor of the two prior frequency discriminators at Fourier frequencies over 1 kHz (compared to the analog PLL discriminator) or 30 kHz (compared to Miteq). The noise floor of the HF2PLL has two contributions, white frequency noise at low Fourier frequency and white phase noise at high frequency. The white frequency noise floor results from white noise in the analog port that outputs the frequency deviation dF. When converted into an equivalent frequency noise using the discriminator sensitivity, this leads to a frequency noise floor that depends on the selected sensitivity D_v and which scales as $1/D_v{}^2$ for D_v below 10 mV/Hz. For higher sensitivities, the frequency noise floor starts to increase again due to other noise contributions. The lowest noise floor is about 3×10^{-8} Hz^2/Hz, obtained for $D_v = 10$ mV/Hz. On the other hand, the white phase noise ($\approx 5 \times 10^{-13}$ rad^2/Hz) at high frequency is due to white noise at the input port of the HF2LI lock-in and is thus insensitive to the PLL output gain. The HF2PLL has the lowest noise floor in the frequency range from 1 Hz to 50 kHz.

4. AM/AN cross-sensitivity

An ideal frequency discriminator should be sensitive to frequency modulation (FM) or frequency noise (FN) only and insensitive to amplitude modulation (AM) or amplitude noise (AN). However, the situation is different in a real device and we have investigated the cross-sensitivity of each discriminator, both in terms of AM and AN. In the first case, a pure AM signal was applied to the input of the discriminator (with an AM depth ranging from 10% to 100% depending on the discriminator) and the output signal was measured using a lock-in amplifier. In the second case, white AN was added at the input of the discriminators and the output voltage PSD was recorded using a FFT analyzer. The sensitivity of each discriminator (in V/Hz) was used to convert the measured AM (AN) response into an equivalent FM (FN) signal. Then, an AM-to-FM (AN-to-FN) conversion factor (in Hz/%) was determined for each discriminator by normalizing the measured equivalent frequency response by the applied AM or AN (this latter was separately measured using a power detector, model Mini-Circuits ZX47-55LN-S+).

Figure 6 shows that all discriminators have some cross-sensitivity to AM and AN, the magnitude of which being very similar in both cases. The analog PLL and the DXD200 show a similar AM (AN) sensitivity, which increases approximately linearly with the modulation frequency, meaning that these discriminators are more sensitive to fast AM (AN). The general trend is similar for HF2PLL, but the AM (AN) sensitivity is two orders of magnitude weaker. Miteq discriminator has by far the highest AM sensitivity with a constant conversion factor of 5 kHz/%.

It was also observed that the AM-to-FM conversion factor in the analog PLL depends somewhat on some loop parameters, such as the amplitude of the input carrier and the servo gain. In this discriminator, the origin of this AM sensitivity lies in some imperfections in the PLL loop, which slightly shift the operating point out of its nominal position. In a perfect analog PLL, the two input signals (LO and RF) are locked in quadrature (90° out-of-phase), as the error signal (mixer output) is zero in this phase condition. In such an ideal situation, it can be demonstrated that a PLL is fully insensitive to

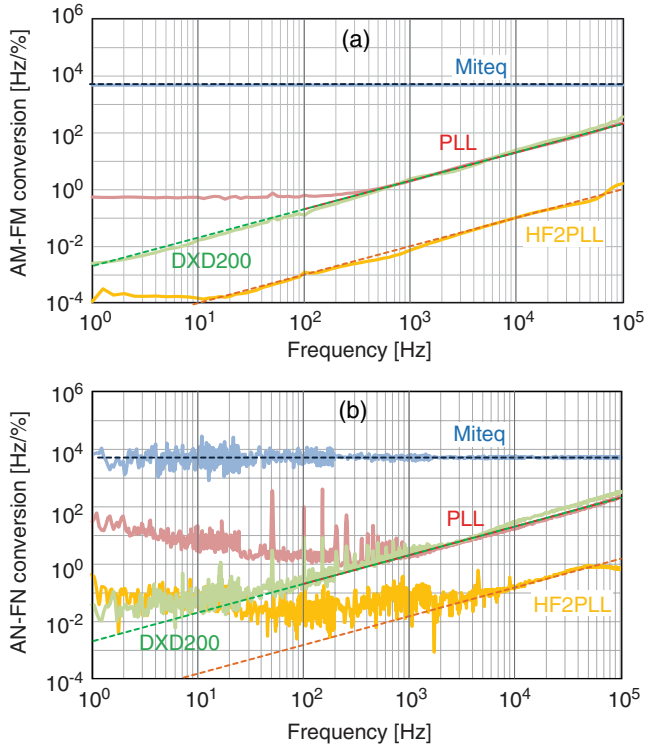

FIG. 6. (Color online) Cross-sensitivity of the discriminators to amplitude modulation (a) and to amplitude noise (b), expressed in terms of AM-to-FM (AN-to-FN) conversion factor (in Hz/%). The dashed lines represent an approximation of the AM–FM (AN–FN) conversion factor as a constant level (for Miteq) or proportional to f (for the other discriminators), obtained in the high frequency range where the measurements are out of the noise floor of each discriminator. These trend lines are used to extract numerical values for the AN–FN cross-sensitivity of each discriminator as listed in Table I.

AM. However, a small electronic offset (e.g., induced at the servo input) may slightly shift the PLL operating point from the quadrature condition, making it sensitive to AM. The response to AM thus directly scales with the small phase shift from the quadrature point. Fine adjustment of the input offset of the PI servo controller allows to retrieve the correct PLL quadrature operation point and to minimize the AM sensitivity compared to the result shown in Fig. 6, obtained without input offset correction. Such adjustment is quite straightforward in presence of pure AM, which is easy to detect, but is more critical in presence of simultaneous AM and FM, or, even worse, in presence of AN and FN.

C. Comparison of the frequency discriminators

Table I summarizes the main properties of each discriminator extracted from the characterization measurements of Sec. II B. A convenient means to compare the characteristics of the different discriminators is to graphically depict their respective domain of application in the plane $(f, S_{\delta\nu})$. The idea is to represent a frequency or phase discriminator as a surface delimited by the following boundaries (Fig. 7(a)): the discriminator noise floor $S_{\min}$, its bandwidth f_{BW}, and the maximum measurable frequency noise PSD $S_{\max}$. While the noise floor and the bandwidth of each discriminator are straightforwardly extracted from the measurements shown in Sec. II B, the upper frequency noise limit has been indirectly determined

TABLE I. Summary of the main properties of the frequency (phase) discriminators. The noise floor is approximated by a power series in f (f^{α}) with up to three different exponents corresponding to flicker frequency noise (range 1, $-2 < \alpha < -1$), white frequency noise (range 2, $\alpha = 0$) and flicker phase noise or white phase noise (range 3, $1 < \alpha < 2$).

	Frequency domain						Noise floor [Hz^2/Hz], $S(f) \sim f^{\alpha}$			
	Total	Linear	Center frequency	Total range	Linear range	Sensitivity	±0.9dB BW	Range 1	Range 2	Range 3	AN–FN conversion
Discriminator	[MHz]	[MHz]	[MHz]	$\Delta f_{\max}$	Δf_{lin}	D_ν	f_{BW} [kHz]	$-2 < \alpha < -1$	$\alpha = 0$	$1 < \alpha < 2$	[Hz/%]
Analog PLL	199–210	203–210	206.5	11 [MHz]	7 [MHz]	7×10^{-7} [V/Hz]	200	$4 \cdot f^{-2}$	10^{-3}	$1 \times 10^{-7} \cdot f$	$2 \times 10^{-3} \cdot f$
HF2PLL	1–49	…	…	$20/D_\nu$ [Hz]	$20/D_\nu$ [Hz]	0.8×10^{-9}–1.6 [V/Hz]	50	…	$3 \times 10^{-12} \cdot D_\nu^{-2}$	$5 \times 10^{-13} \cdot f^2$	$1.5 \times 10^{-5} \cdot f$
Miteq	16–30	18–27	22.5	14 [MHz]	9 [MHz]	1.25×10^{-6} [V/Hz]	2000	$10 \cdot f^{-1}$	10^{-1}	…	5×10^3
DXD200	≈0.5–200	…	…	128π [rad]	128π [rad]	0.018 [V/rad]	1000	…	…	$1.5 \times 10^{-7} \cdot f^{1.3}$	$2 \times 10^{-3} \cdot f$

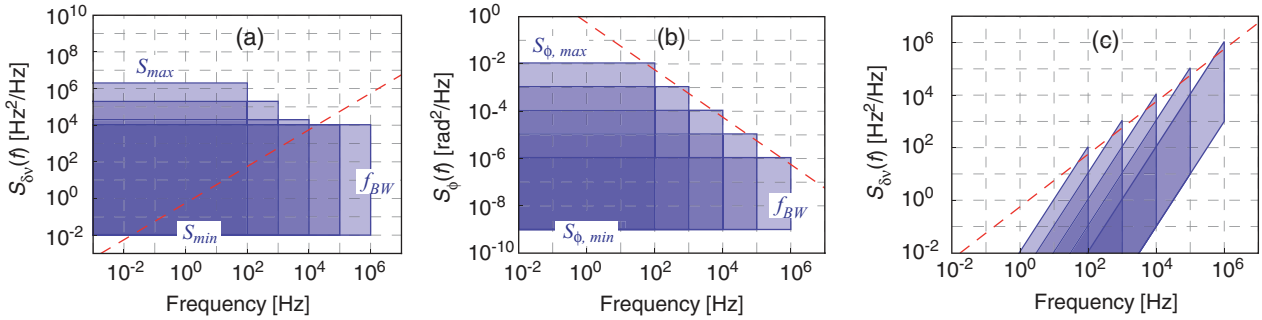

FIG. 7. (Color online) Examples of a graphical representation of a frequency/phase discriminator with different bandwidths ($f_{\rm BW}$ = 100 Hz, 1 kHz, 10 kHz, 100 kHz, 1 MHz): (a) frequency discriminator in the plane (f, $S_{\delta\nu}$), (b) phase discriminator in the plane (f, S_ϕ), and (c) phase discriminator in the plane (f, $S_{\delta\nu}$). The frequency discriminator has a range of $\Delta f = 100$ kHz and a noise floor $S_{\rm min} = 0.01$ Hz^2/Hz; the phase discriminator has a range $\Delta\phi = 2\pi$ and a noise floor $S_{\phi\,\rm min} = 10^{-9}$ rad^2/Hz. The dashed line represents the β-separation line ($S_{\delta\nu} = (8{\rm Ln}(2)/\pi^2)\cdot f$) in the frequency noise spectrum and its correspondent ($S_\phi = (8{\rm Ln}(2)/\pi^2)/f$) in the phase noise spectrum.

from the discriminator linear frequency range $\Delta f_{\rm lin}$, taking into account the relationship that links the frequency noise spectrum and the linewidth. This relation has been discussed in detail in the work of Di Domenico *et al.*[9] and we only summarize here the main conclusions of this study: the frequency noise spectrum $S_{\delta\nu}(f)$ can be divided into two surfaces (the slow and fast modulation areas) by the β-separation line defined as $S_{\delta\nu}(f) = (8{\rm Ln}(2)/\pi^2)\cdot f$. It was shown in Ref. 9 that only the slow modulation area of surface A, for which $S_{\delta\nu}(f) > (8{\rm Ln}(2)/\pi^2)\cdot f$, contributes to the linewidth of the signal, FWHM $= \sqrt{8{\rm Ln}(2)A}$, while the fast modulation area ($S_{\delta\nu}(f) < (8{\rm Ln}(2)/\pi^2)\cdot f$) only contributes to the wings of the lineshape without affecting the linewidth.

A correct measurement of the frequency noise of a beat signal requires that the linewidth of the analysed signal be narrower than the discriminator linear range: FWHM $\ll f_{\rm lin}$. To have a sufficient margin, we request that FWHM $\leq \Delta f_{\rm lin}/n$ and we consider $n = 3$. In this condition, the fraction of the spectral power which is out of the discriminator operating range can be shown to be 0.04% for a Gaussian lineshape (valid for $(8{\rm Ln}(2)/\pi^2)\cdot f_{\rm BW} < S_{\rm max}$, see Ref. 9) and 21% for a Lorentzian lineshape (valid for $(8{\rm Ln}(2)/\pi^2)\cdot f_{\rm BW} > S_{\rm max}$). Assuming a white frequency noise in a bandwidth $f_{\rm BW}$, $S_{\delta\nu}(f < f_{\rm BW}) = S_{\rm max}$, the surface of the slow modulation area is simply $A = S_{\rm max}\cdot f_{\rm BW}$ = FWHM^2/8Ln(2), so that $S_{\rm max} \leq (\Delta f_{\rm lin}/n)^2/(8{\rm Ln}(2) f_{\rm BW})$. For a given discriminator range $\Delta f_{\rm lin,}$ the maximum measureable frequency noise thus decreases as the inverse of the discriminator bandwidth $f_{\rm BW}$. This relation is valid as long as $S_{\rm max} > (8{\rm Ln}(2)/\pi^2)\cdot f_{\rm BW}$. When $S_{\rm max} < (8{\rm Ln}(2)/\pi^2)\cdot f_{\rm BW}$, $S_{\rm max}$ becomes independent of the bandwidth, $S_{\rm max} = \Delta f_{\rm lin}/(n\pi)$. This results from the fact that the additional frequency noise occurring in a bandwidth increment does not contribute to the signal linewidth, as it is entirely below the β-separation line.[9] The upper limit $S_{\rm max}$ of the frequency discriminators has been determined for a white frequency noise; however, one has to keep in mind that a higher frequency noise level acting in a narrower bandwidth would still be measurable if its surface A was smaller than $S_{\rm max}\cdot f_{\rm BW}$.

The geometrical illustration of the phase discriminator is slightly different, as it first has to be represented in the phase noise plane (f, S_ϕ). In that plane, the discriminator is also depicted by a rectangular surface, limited by the following boundaries (Fig. 7(b)): the discriminator noise floor $S_{\phi,\rm min}$, its bandwidth $f_{\rm BW}$, and the maximum measurable phase noise $S_{\phi,\rm max}$. As for the frequency discriminators previously considered, the maximum measurable phase noise $\Delta\phi_{\rm rms}$ must be smaller than the discriminator linear range $\Delta\phi_{\rm lin}$: $\Delta\phi_{\rm rms} \leq \Delta\phi_{\rm lin}/(2n)$ and we again choose $n = 3$. Assuming a low-pass filtered white phase noise $S_\phi(f < f_{\rm BW}) = S_{\phi\rm max}$, the rms phase fluctuations are given by the integrated phase noise $\Delta\phi^2_{\rm rms} = \int_0^{f_{\rm BW}} S_\phi(f)df$ $= S_{\phi\,\rm max}\cdot f_{\rm BW}$, so that $S_{\phi\,\rm max} \leq (1/f_{\rm BW})(\Delta\phi_{\rm lin}/2n)^2$. To have a constant phase excursion $\Delta\phi_{\rm rms}$, the maximum phase noise PSD must be inversely proportional to the discriminator bandwidth. In order to compare the frequency and phase discriminators in the same plot, the rectangular surface representing the phase detector in the plane (f, S_ϕ) is converted into the (f, $S_{\delta\nu}$) plane by applying the transformation (f, $S_\phi(f)$) $\rightarrow$ (f, $f^2\cdot S_\phi(f)$), as $S_{\delta\nu}(f) = f^2\cdot S_\phi(f)$. The constant lower and upper phase noise limits of the phase discriminator thus convert into lines of slope +2 in terms of frequency noise (Fig. 7(c)). One also notices that the maximum frequency noise value moves parallel to the β-separation line as a function of the discriminator bandwidth, as it corresponds to $S_{\rm max} = S_{\phi\,\rm max}\cdot f^2_{\rm BW} = \Delta\phi_{\rm rms}\cdot f_{\rm BW}$ and is thus proportional to the Fourier frequency like the β-separation line. From this observation, one can deduce the phase fluctuations that correspond to the β-separation line: $\Delta\phi_{\rm rms} = \sqrt{8{\rm Ln}(2)}/\pi$ $\cong 0.75$[rad].

The graphical comparison of the different discriminators is shown in Fig. 8. One notices that the analog PLL-discriminator and the Miteq RF discriminator have very similar properties in terms of minimum and maximum measurable frequency noise (slightly better for the analog PLL), but the Miteq discriminator has a wider bandwidth. Their noise floor below the 1 Hz^2/Hz level over a wide frequency range and their intersection with the β-separation line at a Fourier frequency of a few hertz should enable these discriminators to characterize beat signals with a few hertz linewidth (assuming a white frequency noise), provided that no other undesirable effect will degrade the noise floor, as might be the case in presence of the amplitude noise

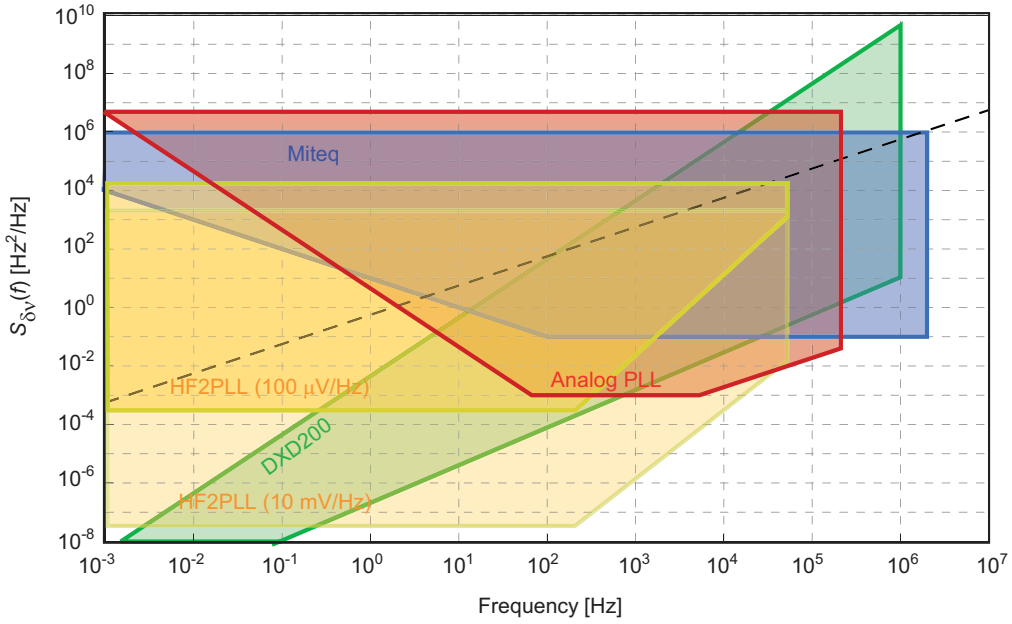

FIG. 8. (Color online) Graphical comparison of the characteristics of the different discriminators. Each discriminator is represented by a surface delimited by its noise floor $S_{\min}$, its bandwidth f_{BW} and the maximum measureable frequency noise PSD $S_{\max}$. The situation for HF2PLL depends on the selected discriminator value D_ν and is shown here for two cases, $D_\nu = 100\ \mu$V/Hz and $D_\nu = 10$ mV/Hz. The dashed line represents the β-separation line $S_{\delta\nu}(f) = (8\mathrm{Ln}(2)/\pi^2)\cdot f$.[9]

(see discussion in Sec. III). The digital phase detector DXD200 enables to detect much smaller frequency fluctuations, especially at low Fourier frequencies, as a result of its sensitivity to the phase fluctuations of the input signal. Owing to its applicability to a large fraction of the slow modulation area which is below the β-separation line, this discriminator is suitable for the characterization of coherent beat signals with sub-radian integrated phase noise. But the maximum frequency noise measurable with this device is limited to $4.5 \times 10^{-3} \cdot f^2$ [Hz^2/Hz] due to its 128π phase coverage.

The HF2PLL combines several advantages of the other discriminators. Its very low-noise performances resulting from the numerical operation convert into a low noise floor, which can be as small as 3×10^{-8} Hz^2/Hz (for $D_\nu = 10$ mV/Hz). This makes the discriminator slightly more sensitive than the DXD200 for the characterization of low-noise beat signals with down to sub-radian integrated phase noise, at Fourier frequencies higher than 100 Hz. However, its bandwidth is slightly lower than for the other discriminators. At lower Fourier frequencies, the HF2PLL discriminator does not compete with the superior capabilities of the digital phase detector DXD200, which results from its white phase noise floor. The flexibility offered by the computer-selectable discriminator value D_ν in the HF2PLL also makes possible the characterization of much wider beat signals with a linewidth ranging from kilohertz to megahertz, which is by far not possible with the digital phase detector. The analog PLL and the Miteq discriminators are also suitable for such broad linewidths.

III. EXAMPLE OF APPLICATION OF THE FREQUENCY DISCRIMINATORS

We present here an example of application of our discriminators for the characterization of a real experimental signal. For illustration purpose, the CEO beat signal of an optical frequency comb is used as a test signal. This CEO-beat is generated from the output of a diode-pumped solid-state 1.56-μm Er:Yb:glass femtosecond laser oscillator, spectrally broadened to an octave spectrum in a highly nonlinear fiber. Details of the frequency comb and generation of the CEO-beat signal can be found in Refs. 20 and 21. Self-referencing of the comb is achieved by stabilizing the CEO-beat, detected in a standard f-to-$2f$ interferometer,[22] to a 20-MHz frequency reference signal using a PLL. The wide linear range of DXD200 digital phase detector, which can track large phase fluctuations of much more than 2π, is used in the PLL to detect the CEO-beat phase fluctuations.

The CEO-beat signal of our comb was used to assess the capability of our different discriminators to measure the frequency noise spectrum of a real signal. Each discriminator was used to demodulate the same 20-MHz CEO signal and the discriminator output signal was measured using a FFT analyzer to determine the frequency noise PSD of the CEO-beat in the range from 1 Hz to 100 kHz. With the analog PLL discriminator, the CEO-beat signal ($f_{\mathrm{CEO}} = 20$ MHz) was mixed with a reference signal ($f_{\mathrm{ref}} = 227$ MHz) in order to frequency up-convert it into the range of operation of this discriminator (at $f_{\mathrm{ref}} - f_{\mathrm{CEO}} = 207$ MHz). With all other devices, the 20-MHz CEO-beat was directly used with an amplitude of 0 dBm. Measurements were performed for the free-running CEO signal and for the CEO phase-locked to a 20-MHz reference signal to reduce its frequency noise. For the stabilized CEO-beat, the digital phase detector DXD200 was used in the stabilization loop to produce the error signal that displays the phase fluctuations of the CEO-beat compared to the reference signal. In that case, the frequency noise PSD measured with the digital phase detector is an in-loop measurement, but it was checked that an out-of-loop measurement performed with a similar device gave an identical result. For all other

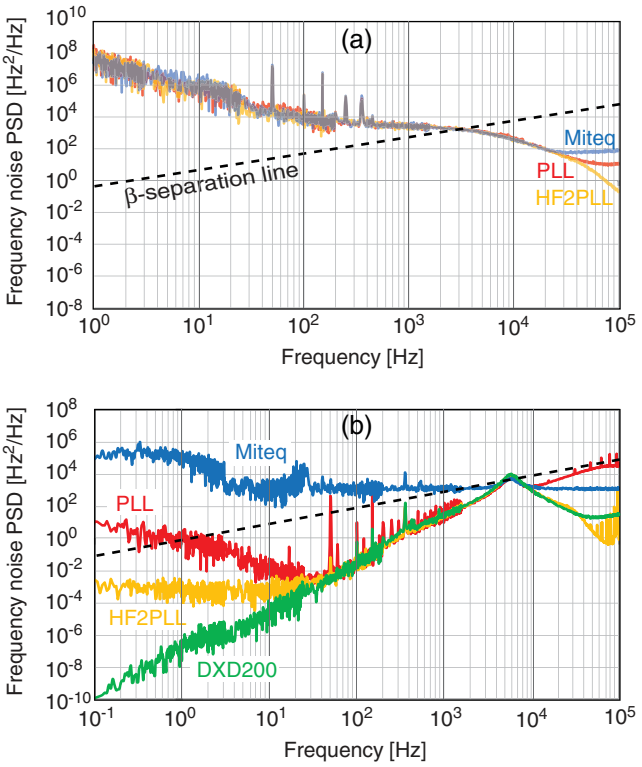

FIG. 9. (Color online) Frequency noise PSD of the CEO-beat in our frequency comb measured with the different discriminators; (a) free-running CEO and (b) CEO phase-stabilized to a 20-MHz reference signal. For HF2PLL, the discriminator value is 100 μV/Hz. The β-separation line that is relevant for the determination of the CEO-beat linewidth is also shown as a dashed line.[9]

discriminators, the frequency noise spectra of the stabilized CEO were measured out-of-loop.

Figure 9 compares the CEO frequency noise spectra obtained with the different discriminators. The free-running CEO-beat has a linewidth (FWHM) of a few kilohertz,[20] measured in an observation time of ≈10 ms. This linewidth is much smaller than the range of operation of all our frequency discriminators (analog and numerical PLLs + Miteq), which are thus perfectly suitable for the characterization of the frequency noise of the free-running CEO-beat. One observes that all the measured spectra are in very good agreement (Fig. 9(a)). However, the digital phase detector DXD200 is not applicable to the measurement of the free-running CEO, as the CEO phase fluctuations are much larger than the range of this discriminator, especially at low Fourier frequency.

The frequency noise is strongly reduced when the CEO is phase-locked to an external frequency reference. A loop bandwidth of ≈5.5 kHz is sufficient to completely reduce the frequency noise of the CEO below the β-separation line, indicating that the CEO-beat linewidth is reduced to zero, resulting in the apparition of a coherent peak in the CEO RF spectrum with a sub-radian integrated phase noise,[23,24] which is the characteristic of a tight phase lock. In that case, the small frequency noise occurring at low Fourier frequencies constitutes a very useful signal for the comparison of the discriminators, as shown in Fig. 9(b). The digital phase detector DXD200 is the most sensitive discriminator at low Fourier frequency, owing to its sensitivity to the phase of the signal rather than to the frequency. The measurement with our analog PLL discriminator overlaps the curve obtained with the digital phase detector in the frequency range $f > 50$ Hz of the spectrum, where significant frequency fluctuations occur as a result of the limited feedback gain and the presence of the loop servo bump. At lower Fourier frequency, the measurement is limited by the noise floor of the analog PLL discriminator.

The HF2PLL should allow to detect lower frequency fluctuations owing to its potentially much lower intrinsic noise floor, which can be reached at elevated discriminator sensitivity D_ν (e.g., $S_{\min} = 3 \times 10^{-8}$ Hz^2/Hz for $D_\nu = 10$ mV/Hz from Sec. II B 3). However, such a high discriminator value could not be used in this measurement and a value $D_\nu = 100$ μV/Hz was used instead. The low frequency noise floor is reduced to $\approx 5 \times 10^{-4}$ Hz^2/Hz in this case, in good agreement with the level observed in the CEO frequency noise spectrum.

Finally, Miteq discriminator can measure only a small portion of the locked CEO frequency noise spectrum due to a high noise floor ($\approx 1 \times 10^3$ Hz^2/Hz) observed with this discriminator out of the servo bump at ≈7 kHz. This is a result of the strong AN cross-sensitivity of this discriminator. In order to stabilize the CEO frequency in our comb, feedback is applied to the femtosecond laser pump power.[24] The CEO frequency stabilization thus results in larger fluctuations of the femtosecond laser output power, and in a higher amplitude noise in the CEO-beat signal. The relative amplitude noise PSD measured in the CEO-beat is ≈ −84 dB/Hz in the range 200 Hz–100 kHz and increases roughly as $1/f$ for $f < 200$ Hz (measured with a power detector). With the measured AN–FN conversion factor of 5 kHz/% for Miteq discriminator, this translates into an AN-induced noise floor of ≈900 Hz^2/Hz, in very good agreement with the observed value of $\approx 1 \times 10^3$ Hz^2/Hz, showing that the measurement with this discriminator is strongly limited by its AN sensitivity.

IV. DISCUSSION AND CONCLUSION

We have described and fully characterized a PLL frequency discriminator developed to analyze the frequency noise properties of a RF signal, e.g., an optical beat signal between two lasers or between a laser and a frequency comb. Owing to its large linear frequency range of 7 MHz, its bandwidth of 200 kHz and its noise floor below 0.01 Hz^2/Hz in the range ≈10 Hz–100 kHz, this frequency discriminator is able to fully characterize the frequency noise of a beat signal with a linewidth ranging from a couple of megahertz down to a few hertz. It thus has a wide range of applications, for instance for the characterization of the frequency noise spectrum of free-running lasers, the measurement of transfer functions in free-running optical frequency combs (for the CEO, the repetition rate or an individual comb line), or for the characterization of the frequency noise properties of stabilized frequency combs and ultra-narrow linewidth cavity-stabilized lasers.

For comparison, we also characterized three other commercially available discriminators of different types, (i) a Miteq RF discriminator, (ii) a numerical PLL (HF2PLL)

encompassed in a high-frequency lock-in amplifier, and (iii) a digital phase detector (DXD200). From their measured characteristics, these discriminators were compared with respect to their respective domain of application in the frequency noise plane (f, $S_{\delta\nu}$). These discriminators have complementary properties that make them applicable to different types of input signals.

The Miteq discriminator is the simplest to use. With its wide linear range of operation, it is perfectly suitable to the characterization of free-running lasers or frequency combs. Its white frequency noise floor of 0.1 Hz^2/Hz reached at $f > 100$ Hz with a $1/f$ increase at lower frequency should make it applicable also for the analysis of narrow-linewidth signals. However, this discriminator has shown a strong sensitivity to amplitude modulation and amplitude noise with a conversion factor of ≈5 kHz/%, which strongly limits its use for low frequency noise signals in presence of amplitude noise. For this reason, this discriminator could only measure a small portion of the frequency noise spectrum of the locked CEO in our frequency comb, the rest of the spectrum being hidden by the AN-induced noise floor.

The HF2PLL has a computer-selectable output gain allowing to achieve a broad range of discrimination factors, and thus to straightforwardly adjust its domain of operation. This flexibility, combined with its low intrinsic noise floor, makes this discriminator applicable to the characterization of lasers with a wide range of linewidths. However, the lower bandwidth of this discriminator prevents a complete characterization of the frequency noise spectrum of lasers with MHz-range linewidth, such as distributed feedback lasers. Furthermore, the potential capability of this discriminator to reach a very low noise floor at low Fourier frequencies, and thus to characterize low-noise beat signals with sub-radian integrated phase noise, is somewhat limited by the impracticality to use a high discriminator factor with a real signal. For this reason, the characterization of the CEO frequency noise in our frequency comb was limited to Fourier frequencies $f > 100$ Hz. At lower frequencies, a noise floor of $\approx 10^{-3}$ Hz^2/Hz, prevents the detection of smaller frequency fluctuations, despite the much lower intrinsic noise floor of the HF2PLL in the 3×10^{-8} Hz^2/Hz range obtained at a higher discriminator factor of 10 mV/Hz.

Finally, the digital phase detector DXD200 is very sensitive to small frequency fluctuations at low Fourier frequency owing to its sensitivity to phase fluctuations, which makes it the most sensitive device for the characterization of a real beat signal containing simultaneous frequency noise and amplitude noise, such as encountered in the frequency-stabilized CEO-beat in our frequency comb.

ACKNOWLEDGMENTS

The authors would like to thank R. Scholten for fruitful discussions about the analog PLL discriminator and Niels Haandbaek for the HF2PLL. The authors are also very grateful to Professor Ursula Keller, ETH Zurich, for making available the optical frequency comb developed in her Laboratory and used here for assessing the frequency discriminators. This work was financed by the Swiss National Science Foundation (SNSF) and by the Swiss Confederation Program Nano-Tera.ch, scientifically evaluated by the SNSF.

[1] C. E. Wieman and L. Hollberg, Rev. Sci. Instrum. **62**(1), 1 (1991).
[2] L. Hollberg, S. Diddams, A. Bartels, T. Fortier, and K. Kim, Metrologia **42**, S105 (2005).
[3] G. P. Barwood, P. Gill, G. Huang, and H. A. Klein, IEEE Trans. Instrum. Meas. **56**, 226 (2007).
[4] J. Alnis, A. Matveev, N. Kolachevsky, Th. Udem, and T. W. Hänsch, Phys. Rev. A **77**, 053809 (2008).
[5] B. C. Young, F. C. Cruz, W. M. Itano, and J. C. Bergquist, Phys. Rev. Lett. **82**, 3799 (1999).
[6] R. W. P. Drever, J. L. Hall, F. V. Kowalski, J. Hough, G. M. Ford, A. J. Munley, and H. Ward, Appl. Phys. B **31**, 97 (1983).
[7] T. Okoshi, K. Kikuchi, and A. Nakayama, Electron Lett. **16**, 630 (1980).
[8] L. D. Turner, K. P. Weber, C. J. Hawthorn, and R. E. Scholten, Opt. Commun. **201**, 391 (2002).
[9] G. Di Domenico, S. Schilt, and P. Thomann, Appl. Opt. **49**, 4801 (2010).
[10] S. Bartalini, S. Borri, P. Cancio, A. Castrillo, I. Galli, G. Giusfredi, D. Mazzotti, L. Gianfrani, and P. De Natale, Phys. Rev. Lett. **104**, 083904 (2010).
[11] S. T. Cundiff and J. Ye, Rev. Mod. Phys. **75**(1), 325 (2003).
[12] L. Tombez, J. Di Francesco, S. Schilt, G. Di Domenico, J. Faist, P. Thomann, and D. Hofstetter, Opt. Lett. **36**(16), 3109 (2011).
[13] G. Galzerano, A. Gambetta, E. Fasci, A. Castrillo, M. Marangoni, P. Laporta, and L. Gianfrani, Appl. Phys B **102**(4), 725 (2011).
[14] J.-P. Tourrenc, "Caractérisation et modélisation du bruit d'amplitude optique, du bruit de fréquence et de la largeur de raie de VCSELs monomode," Ph.D. dissertation (Université de Montpellier II, 2005).
[15] D. M. Baney and W. V. Sorin, "High Resolution Optical Frequency Analysis," in *Fiber Optic Test and Measurements*, edited by D. Derickson (Prentice Hall, New Jersey, 1998), Chap. 5.
[16] See http://www.miteq.com/products/discriminators/frequency-discriminators.php for additional informations about RF Miteq discriminators.
[17] See http://www.zhinst.com/products/hf2pll for additional information about the HF2PLL discriminator.
[18] M. Prevedelli, T. Freegarde, and T. W. Hänsch, Appl. Phys. B **60**(2–3), S241 (1995).
[19] E. Rubiola, "The Leeson effect - Phase noise in quasilinear oscillators," in *Phase Noise and Frequency Stability in Oscillators* (Cambridge University Press, Cambridge, 2008), Chap. 3.
[20] M. C. Stumpf, S. Pekarek, A. E. H. Oehler, T. Südmeyer, J. M. Dudley, and U. Keller, Appl. Phys. B **99**(3), 401 (2010).
[21] M. Stumpf, S. Pekarek, A. E. H. Oehler, T. Südmeyer, J. M. Dudley, S. Schilt, G. Di Domenico, P. Thomann, and U. Keller, "First fully stabilized frequency comb from a SESAM-modelocked 1.5 μm solid-state oscillator,"in *Proceedings of EFTF 2010, 24th European Frequency and Time Forum*, Noordwijk, The Netherland, 13–16 April 2010.
[22] H. R. Telle, G. Steinmeyer, A. E. Dunlop, J. Stenger, D. H. Sutter, and U. Keller, Appl. Phys. B **69**, 327 (1999).
[23] S. Schilt, V. Dolgovskiy, N. Bucalovic, L. Tombez, M. C. Stumpf, G. Di Domenico, C. Schori, S. Pekarek, A. E. H. Oehler, T. Südmeyer, U. Keller, and P. Thomann, "Optical frequency comb with sub-radian CEO phase noise from a SESAM-modelocked 1.5-μm solid-state laser," CLEO-2011, Baltimore, USA, 1–6 May 2011, Paper CFK3.
[24] S. Schilt, N. Bucalovic, V. Dolgovskiy, C. Schori, M. C. Stumpf, G. Di Domenico, S. Pekarek, A. E. H. Oehler, T. Südmeyer, U. Keller, and P. Thomann, Opt. Express **19**(24), 24171 (2011).